Hindawi
Journal of Nanomaterials
Volume 2022, Article ID 1653449, 17 pages
https://doi.org/10.1155/2022/1653449

Research Article

Influence of Nanoclay Filler Material on the Tensile, Flexural, Impact, and Morphological Characteristics of Jute/E-Glass Fiber-Reinforced Polyester-Based Hybrid Composites: Experimental, Modeling, and Optimization Study

B. A. Praveena,[1] N. Santhosh,[2] D. P. Archana,[3] Abdulrajak Buradi,[1] E. Fantin Irudaya Raj,[4] C. Chanakyan,[5] Ashraf Elfasakhany,[6] and Dadapeer Basheer[7]

[1]*Department of Mechanical Engineering, Nitte Meenakshi Institute of Technology, Bangalore, 560064 Karnataka, India*
[2]*Department of Mechanical Engineering, MVJ College of Engineering, Bangalore, 560067 Karnataka, India*
[3]*Department of Civil Engineering, Bangalore Institute of Technology, Bangalore, 560004 Karnataka, India*
[4]*Department of Electrical and Electronics Engineering, Dr. Sivanthi Aditanar College of Engineering, Tiruchendur, 628 215 Tamil Nadu, India*
[5]*Department of Mechanical Engineering, Government College of Engineering, Sengipatti, Thanjavur, 613402 Tamil Nadu, India*
[6]*Mechanical Engineering Department, College of Engineering, Taif University, P.O. Box 11099, Taif 21944, Saudi Arabia*
[7]*Department of Mechanical Engineering Haramaya Institute of Technology, Haramaya University, Dire Dawa, Ethiopia*

Correspondence should be addressed to Dadapeer Basheer; dadapeer.basheer@haramaya.edu.et

Received 17 March 2022; Accepted 25 May 2022; Published 15 June 2022

Academic Editor: Palanivel Velmurugan

The use of natural fibers as reinforcement in polymer composite materials is increasing owing to the ecocompatibility. The fabrication of natural fiber-based composite is now an emerging field of study, and it is the most desired choice not only because of its superior qualities such as light weight, stiffness, and low density but also because of being economical and renewable. However, the mechanical characteristics of these composites are a major concern and thus require some additives in the form of nanoclay, which can readily act as a filler material, thereby enhancing the tensile, flexural, and impact strengths of the natural fiber composites. In this regard, a hybrid polymer composite with jute and E-glass fiber as reinforcements, along with Cloisite 20 nanoclay filler material, is fabricated by a hand layup process in a steel mold box and cut to the ASTM standards. The composition of the reinforcements is fixed based on the initial experimental studies and review of the literature findings. The wt.% of jute is fixed in the range of 10 wt.% to 20 wt.% with 5 wt.% interval for each composition, while the wt.% of E-glass fiber varied from 10 wt.% to 30 wt.% with 10 wt.% interval and that of the Cloisite 20 nanoclay filler varied from 2 wt.% to 6 wt.%. The fabricated composite specimens with varying wt.% of reinforcements and nanofiller material are subjected to standard tests for evaluating their mechanical characteristics viz., the tensile, flexural, and impact strength and the morphological characteristics. The results of the experiments have revealed that combining natural and synthetic fibers in a composite increases the impact, tensile, and flexural strength of the material. That is, the composite specimens fabricated with 20 wt.% of jute fiber and 20 wt.% of E-glass fiber and 2 wt.% of Cloisite 20 nanoclay have the maximum tensile strength of 69.7 MPa, tensile modulus of 3816.43 MPa, and impact strength of 178.62 J/m^2 and flexural modulus of 275.15 MPa among all the specimens, while the composite specimen fabricated with 20 wt.% of jute fiber and 30 wt.% of E-glass fiber and 4 wt.% of the filler material possesses the maximum flexural strength of 90.22 MPa. This is also ascertained from Taguchi's optimization studies and statistical model (regression equations) developed.

1. Introduction

Natural fiber-reinforced composites are a modern class of engineering materials used profusely because of their eco-compatibility and cost considerations. They are partially recyclable and biodegradable. The interest in this field is increasing with regard to the engineering applications, and several investigations are carried out [1, 2]. Jute seems to be an encouraging natural fiber reinforcing material, since it is moderately economical and commercially accessible among all natural fiber reinforcing materials [3, 4]. E-glass fiber-reinforced polymers are unique combination of composite materials used majorly in all the engineering domains, because of their excellent properties. Fiber glass is a tough reinforcement used in fabrication of various composites [5–7]. In the elongation property, there is a positive hybrid effect. Glass and hybrid fiber reinforcement in phenol formaldehyde resin caused in an economical, insubstantial composite with better performance characteristics. These composites could be used in structural applications where strength and cost are significant [8]. Industrialists and designers may now combine shapes and materials in new ways to improve efficiency of composite structures. They have a lot of future growth potential, in addition to being lightweight, durable, and flexible [9]. These materials have advanced specific strength than nonmetals, metals, and even alloys, as well as a lower specific gravity, improved creep and fatigue resistance, corrosion, and oxidation resistance [10]. They are used in a selection of applications, including automotive (shafts and hulls), marine, aeronautical (rocket components), and aircraft and safety equipment (ballistic protection and airbags). The matrix and reinforcement efficiency are what determines how well these materials perform [11, 12]. The most commonly used matrices in composites are thermoset resins, such as polyester, which can replace very costly steels and alloys [13, 14]. They have high basic strength and stiffness, good fatigue behavior, limited corrosion, and chemical and environmental resistance. They are both simple to patch and magnetically insensitive. Fiber- or particle-reinforced composites are potential choices. Jute, bamboo, banana, and other natural fibers are vastly available in tropical countries. These natural fiber-reinforced composites are illustrious for their unique properties, such as lightweight, environmental friendliness, biodegradability, low cost, abundant availability, sustainability, low density, and strength, which make them superior to traditional materials [15–17]. Mechanical properties of jute/glass fiber-reinforced polyester hybrid composites are reported to be enhanced by the inclusion of nanofiller [18]. The hybrid effect of glass/jute fiber composites developed by hand layup using polyester resin and hardener is reported by researchers. The test results show that the properties of the hybrid jute/glass fiber composite are much superior to those of the jute fiber composite [19, 20]. Other studies revealed that the jute polyester with an aluminum metal powder composite panel has a greater tensile strength than the jute polymer composite panel, according to the experimental findings [21, 22]. Similar studies [23–25] show greater tensile strength of manufactured composites due to the higher weight percent of reinforced fiber. With the incorporation of jute fiber, the composites perform like a ductile as well as semibrittle material. As a result, composite specimens outlast pure coir specimens on a fundamental basis. Although combining two natural fibers to create a hybrid composite has the advantage of being able to substitute synthetic fibers, this research also demonstrates that hybrid natural fiber composites can be used as a lightweight material with relatively reduced strength characteristics [26]. Natural fiber-reinforced polymer composites have recently gained significant attention due to the collective comprehensive ecocompatibility. Natural fiber-reinforced polymer composites have a significant effect on research areas due to their accessibility, environmental friendliness, biodegradability, high specific properties, renewability, strong acoustic and thermal properties, superior energy recovery property, nonabrasive design, and low energy consumption [11, 15]. Jute fiber seems to be the most beneficial, affordable, and commercially viable natural fiber, capable of being formed into a uniform scale and complex shaped elements by using their fascinating strengthening ability [4]. Jute fibers have a multicellular arrangement made up of microfibrils, and the texture is extremely irregular [27], with properties that vary significantly, based on its geographic origin, environment, biochemical composition, molecular structure features, and physical state and processing methods [15, 28]. Despite its cost and availability, jute fiber reinforcement has a number of drawbacks, including poor fiber matrix adhesion, poor wet ability, inherent separation due to the inclusion of carboxyl and hydroxyl assemblies in its arrangement, and low humidity resistance [28]. Many efforts to relieve these forms of congestions, such as physical and chemical therapies, result in improvements to the fiber strength. An option for improvement of such fiber strength is hybridization with synthetic fibers and inclusion of nanofillers. The mechanical properties of a composite made of glass and fiber with nanoclay filler materials are superior to those of traditional composites. It is also a natural material that is partly ecofriendly [29, 30]. Researchers' interest in polyester-based composite materials has grown in recent years as an outcome of their toughness and improved mechanical properties, such as increased surface stiffness, tensile strength, and improved insulating properties. Natural fibers, on the other hand, have some disadvantages, such as poor tensile strength, low resilience, and the propensity to degrade quickly, but when used in the right proportions with synthetic materials like polyester and glass fiber, these disadvantages can be overcome. Further, the inclusion of the nanofiller materials has significant influence on the mechanical characteristics of the composite specimens. The nanofiller materials bring about inoculation in the composite materials and improve the bonding between the matrix and the reinforcement. This further improves the mechanical characteristics of the composite specimens [31]. Thorough review of the available literature has provided a research gap for carrying out the research in the domain of hybrid polymer composites reinforced with natural and synthetic fibers. From the review, it is learned that the natural fiber-reinforced composites have considerably lower mechanical properties as compared

to the synthetic fiber-reinforced composites. Also, the synthetic fiber-reinforced composites are subject to delamination and interlaminar shear failure. However, these problems can be overcome by hybridization. Hybrid composites are also prone to the problems of aggregation and localized agglomeration, which can be overcome by the use of nanofillers. Thus, the present work is focused on the development of jute-E-glass fiber-reinforced hybrid polyester composites with Cloister 20 nanoclay filler material for enhanced tensile, flexural, and impact characteristics.

2. Materials and Experimental Details

2.1. Materials. Jute and E-glass fibers were used as reinforcements in this research work, and the polyester resin served as the matrix. To boost interfacial bond and impart strength to the composites, hardeners were used. The HP-21 polyester resin and the Methyl Ethyl Ketene Polyester (MEKP) Hardener and E-glass fibers were procured from S & S Impel, Bangalore, Karnataka State, India. The woven jute mat was purchased at a nearby marketplace of Bindiganavile village, Karnataka State, India. To achieve the best matrix composition, a 3 : 1 resin and hardener combination was used along with the Cloister 20 Metal Montmorillonite-(MMT-) based nanoclay powder sourced from the Ultra Nano Tech Pvt. Ltd., Hoodi Industrial Area, Bangalore City, Karnataka State, India. Table 1 gives the physical properties of jute fiber, E-glass fiber, and polyester resin as reported in the supplier specification manuals. Figure 1 shows the (a) Glass fiber (b) Jute fiber and (c) Polyester resin used for the present work.

2.2. Composite Fabrication. A hybrid of jute/E-glass fiber-reinforced polyester was used in an attempt to fabricate composites. Hand layup process is used to make composites a steel mold box with a cross section of $250 \times 150\,mm^2$ and a thickness of 3 mm. All of the mold surfaces are coated with a wax coat that serves as a release agent. The bottom of the mold is covered with a mixture of liquid resin and hardener, followed by a 1 mm layer of E-glass fiber (reinforcement). The resin is impregnated and distributed evenly around the surface using a roller. Another layer of resin and reinforcement is added until the thickness reaches 3 mm. A 1 mm thick jute fiber is packed between two glass fibers in a hybrid composite. The mold is left to cure in the sun for a week before being removed. Table 2 shows the specimen compositions.

The composition of the reinforcements for the fabrication of the composites is considered based on the initial trials of the experiments and the review of the literature findings. Also, the weight fraction of the jute fibers is fixed in the range of 10 wt.% to 20 wt.%, with an interval of 5 wt.%. While the weight fraction of the E-glass fibers is fixed in the range of 10 wt.% to 30 wt.%, with an interval of 10 wt.%, and the weight fraction of Cloisite 20 nanoclay filler material is fixed in the range of 2 wt.% to 6 wt.% with an interval of 2 wt.%. The range is selected based on the minimum and maximum variations in the properties based on the observation of the initial set of trials and the variance for each set of composition on either side of the mean. Further, it is noted that the variation of the properties is predominant in the range of the reinforcements and the filler selected. Apart from the improvements in the properties, due considerations also need to be given to the agglomeration, void formations, and bonding between the matrix and reinforcements, since the increase in the weight fraction of the reinforcements beyond 50 wt.% and the increase in the weight fraction of the filler material beyond 6 wt.% may lead to agglomeration and subsequent reduction in the characteristics of the composites.

Table 1: Physical properties of jute, glass, and polyester resin [13, 16].

Properties	Jute fiber	E-glass fiber	Polyester resin
Density (gm/cm^3)	1.30-1.46	2.46-2.60	1.2
Elongation (%)	1.5-1.8	4.8-5.7	2-3
Tensile strength (MPa)	398-800	3400-4900	50-65
Young's modulus (GPa)	10-30	68-87	3

2.3. Mechanical Testing. The tensile test is carried out by cutting the composite sample in compliance with ASTM D638 (specimen dimensions are $250 \times 25 \times 3\,mm^3$). A universal testing machine (Make: Fine Instruments, Model: TFUC-600) is used for testing with an extreme load rating of 1500 N [13]. Figure 2(a) shows the sample of the tensile test specimen. In every casing, three specimens are examined, and the standard is calculated and recorded. The displacements of the sample are measured after a load is applied on it. The break load and tensile strengths are measured before the sample fails. According to the standard ASTM D790, the flexural evaluation is conducted in a three-point flexural configuration [14]. When a weight is added to the center of the sample, it bends and splits. This flexural test is carried out in the UTM. Figure 2(b) shows the sample of the flexural test sample. In compliance with ASTM D256, specimens were prepared (sample size is $65 \times 12.5 \times 3\,mm^3$) and tested in the impact test performed in a Charpy impact machine (Make: Fine Instruments, Model: TFIT-300). The specimen must be placed into the measuring system, and the pendulum must be allowed to swing before the specimen breaks. The energy required to break the material is calculated using the impact test. The hardness and yield force of a substance are determined by this test. The impacts of strain rate on the fracturing and flexibility of a material are studied. Figure 2(c) shows the sample of the impact test specimen.

2.4. Microscopy. The exterior of processed and untreated fibers, as well as the broken surfaces of tensile, flexural, and impact test samples, is analyzed using an emission scanning electron microscopy (SEM) working at 4 kV. Specimens were carbon taped to aluminum ends before being sputter covered with platinum and palladium to make them conductive for scanning electron microscopy analysis.

Glass fiber

(a)

Jute fiber

(b)

Polyester resin

(c)

Figure 1

Table 2: Specimen compositions.

Specimen designation	Jute (wt.%)	E-glass fiber (wt.%)	Cloister 20 nanoclay (wt.%)	HP-P21 polyester resin	MEKP hardener
S1	10	10	2	58.5	19.5
S2	10	20	4	49.5	16.5
S3	10	30	6	40.5	13.5
S4	15	10	4	53.25	17.75
S5	15	20	6	44.25	14.75
S6	15	30	2	39.75	13.25
S7	20	10	6	48	16
S8	20	20	2	43.5	14.5
S9	20	30	4	34.5	11.5

3. Results and Discussions

3.1. Tensile Test. The tensile testing in UTM determines the tensile characteristics of the composite specimens. Table 3 illustrates the tensile strength and tensile modulus values for composites. The integration of glass fabric as the skin layer or outside ply results in a progressive rise in tensile characteristics. The hybrid composites with optimum wt.% of nanofiller material are found to have higher tensile strength and modulus values among all the other set of composites correspondingly, indicating that the tensile properties of two natural fibers with glass fibers are more than single natural fibers. As a result of all of these findings, it is obvious that the composite's tensile strength is controlled by the modulus and strength of all hybridized fibers. The addition of glass fiber enhances the composite tensile qualities, and combining jute and glass fibers improves the composites' ability to survive additional tensile weight, when combining single natural fibers with glass fibers. According to ASTM D3038 standards, a tensile test was performed in a UTM to determine the tensile strength of jute/E-glass polymer hybrid composites. As can be seen from the results, the optimum result obtained was for S8 specimen. The tensile property findings demonstrate that the greatest strength functional to the hybrid composites was 752 N before the specimen fractured. The material's maximum displacement was 1.18 mm for S8 hybrid composite specifications. The experimental results obtained from the tensile tests to determine the ultimate tensile strength and the tensile modulus are given in Table 3. Figure 3 shows the tensile strength of the specimens.

Further, the experimental outcomes are statistically validated using Taguchi's techniques to determine the optimum factor levels for maximizing the tensile strength out of the combinations selected for the present work. Taguchi's optimization is carried out in accordance with the "larger is better" option with the S/N ratio dependent on the response factor and the combinations of the levels.

$$\frac{S}{N} = -10 * \log\left(\frac{\Sigma\left(1/Y^2\right)}{n}\right), \tag{1}$$

where Y is the responses for the given factor level combination and n is the number of responses in the factor level combination.

3.2. Tensile Strength. Tensile strength is an important attribute for evaluating the performance characteristics of the composite specimens. The tensile strength is maximum (74.58 MPa) for the S9 composite specimen with 20 wt.% of jute fiber and 30 wt.% of E-glass fiber and 4 wt.% of Cloisite 20 nanoclay filler material. The inclusion of nanoclay filler material improves the bonding strength between the

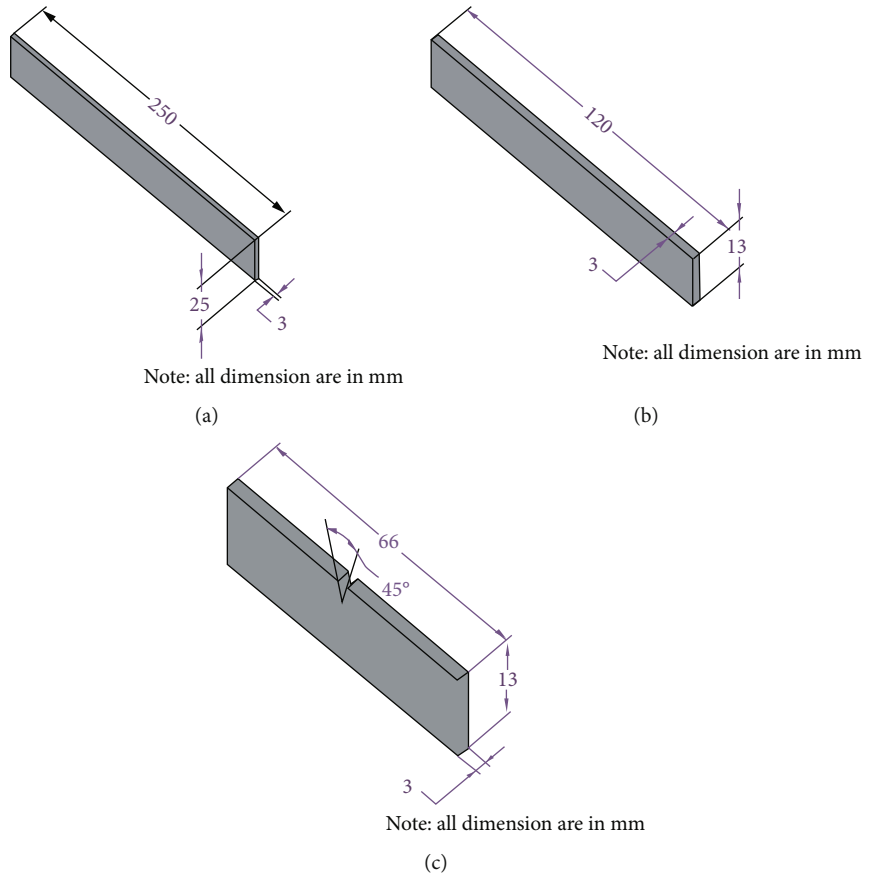

Figure 2: Test samples prepared as per ASTM standards: (a) tensile test specimen; (b) flexural test specimen; (c) impact test specimen.

Table 3: Results of the tensile test.

Specimen designation	Jute (wt.%)	E-glass (wt.%)	Cloisite 20 nanoclay (wt.%)	Tensile strength (MPa)	Tensile modulus (MPa)
S1	10	10	2	49.56	3156.45
S2	10	20	4	55.45	3215.44
S3	10	30	6	58.65	3256.3
S4	15	10	4	57.96	3489.65
S5	15	20	6	57.56	3356.21
S6	15	30	2	58.23	3456.28
S7	20	10	6	60.12	3552.57
S8	20	20	2	69.7	3816.43
S9	20	30	4	74.58	2689.61

reinforcements and the matrix phase. The findings of the present work are in line with the inferences drawn by Ravichandran et al. [32] who have studied the influence of the nanofiller materials on the composite specimens. They have reported that the inclusion of the nanofiller will facilitate microcoring and segregation and improve the tensile strength of the composite specimens due to coherent bonding. This is also ascertained from Taguchi's optimization and the response tables and response plots.

The response table for SN ratios as shown in Table 4 and means as shown in Table 5 for tensile strength is critically evaluated, and from the evaluation, it is herewith noted that the wt.% of jute fiber is having a major influence on the tensile strength, subsequently followed by the wt.% of E-glass fiber and wt.% of cloister 20 nanoclay.

Further, the response table for means gives an overview of the means for the combination of the control factors considered in the design of experiments for maximizing the tensile strength of the composite specimens.

Figure 4 gives the main effects plot for SN ratios, while Figure 5 gives the main effects plot for means. The main effects plot for SN ratios and the mean of means clearly indicate that the control factors can be optimally discerned with the level 3 of wt.% of jute (A3), level 3 of wt.% of E-glass fiber (B3), and level 2 of wt.% of Cloister 20 nanoclay (C2). Thus, The S/N ratio and mean of means analysis suggests that the A3, B3, and C2 are the optimum levels for maximizing the tensile strength for the hybrid polymer composites.

Further, the response (tensile strength) and control factors are considered to model the influence of factors. From the statistical modeling of the responses and factors,

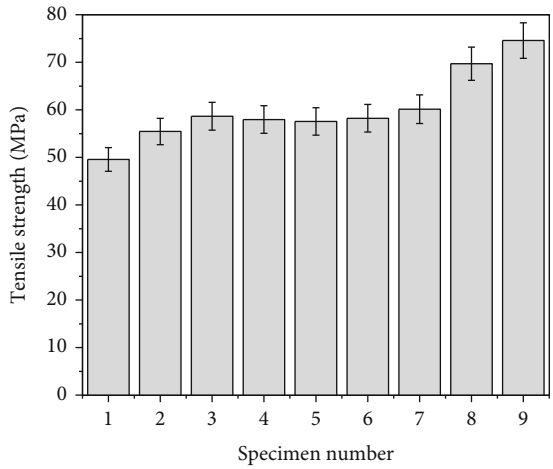

Figure 3: Tensile strength of specimens.

Table 4: Response table for signal to noise (S/N) ratios for tensile strength (MPa).

Level	Jute (wt.%)	E-glass fiber (wt.%)	Cloisite 20 nanoclay (wt.%)
1	34.72	34.92	35.36
2	35.26	35.65	35.86
3	36.63	36.04	35.38
Delta	1.92	1.13	0.51
Rank	1	2	3
Larger is better			

Table 5: Response table for means for tensile strength.

Level	Jute (wt.%)	E-glass fiber (wt.%)	Cloisite 20 nanoclay (wt.%)
1	54.55	55.88	59.16
2	57.92	60.90	62.66
3	68.13	63.82	58.78
Delta	13.58	7.94	3.89
Rank	1	2	3

equation (2) is obtained, which can be effectively used to predict the tensile strength for different wt.% of reinforcements and the filler content.

$$\text{Tensile Strength (MPa)} = \exp\left(Y'\right),$$

$$Y' = 3.620 + 0.0226 * \text{Jute(wt.\%)} + 0.00660 * \text{E-Glass Fiber (wt.\%)} + 0.0002 * \text{Cloisite 20 Nanoclay (wt.\%)}. \quad (2)$$

Figures 6 and 7 give the surface and 3D contour plots for the varying wt.% of reinforcements for 4 wt.% of Cloister 20 nanoclay (optimized wt.%). It is evident from the graphs that the tensile strength increases in the range of 50 MPa to 70 MPa with the increase in the E-glass fiber content from 10 wt.% to 30 wt.% and the jute fiber content from 10 wt.% to 20 wt.%. This is attributed to the increased load carrying capacity of the composites with the inclusion of fibers and

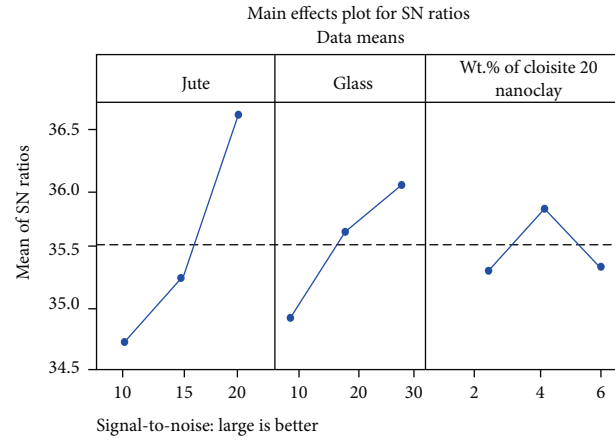

Figure 4: Main effects plot for SN ratios for tensile strength.

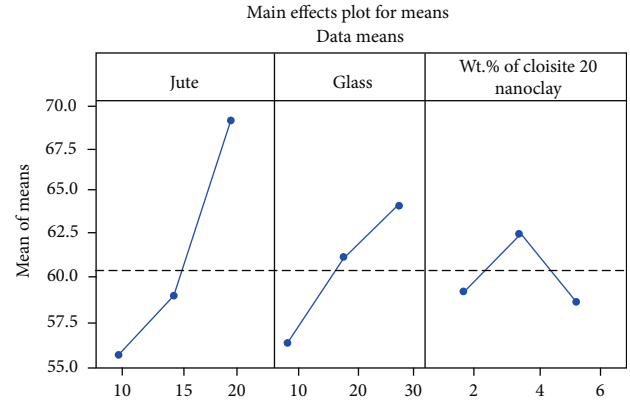

Figure 5: Main effects plot for means for tensile strength.

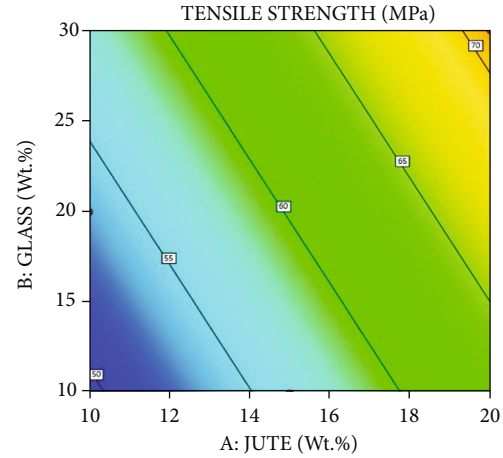

Figure 6: Surface plots for varying wt.% of jute and E-glass fiber for tensile strength for the composite specimens with 4 wt.% nanofiller (optimized wt.%).

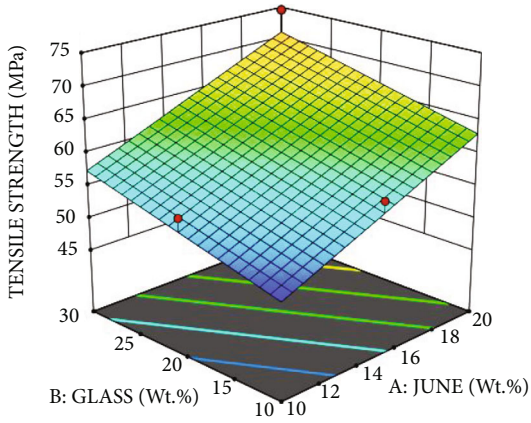

Figure 7: 3D contour plot for varying wt.% of jute and E-glass fiber for 4 wt.% nanofiller (optimized wt.%).

Table 6: Response table for signal to noise (*S*/*N*) ratios for tensile modulus.

Level	Jute (wt.%)	E-glass fiber (wt.%)	Cloisite 20 nanoclay (wt.%)
1	70.13	70.62	70.80
2	70.71	70.76	69.86
3	70.41	69.87	70.59
Delta	0.59	0.89	0.93
Rank	3	2	1
Larger is better			

Table 7: Response table for means for tensile modulus.

Level	Jute (wt.%)	Glass fiber (wt.%)	Cloisite 20 nanoclay (wt.%)
1	3209	3400	3476
2	3434	3463	3132
3	3353	3134	3388
Delta	225	329	345
Rank	3	2	1

strong bonding brought about by the optimum content of nanofiller material.

3.3. Tensile Modulus. The tensile modulus gives the measure of the stiffness of the composite laminate. The tensile modulus is an important parameter for the composite materials. From the experiments, the tensile modulus is found to be maximum (3816.43) for the S8 specimen having 20 wt.% of jute fiber and 20 wt.% of E-glass fiber and 2 wt.% Cloisite nanofiller. This is also ascertained from the response table as shown in Table 6 for SN ratios and means as shown in Table 7 for tensile modulus, and from the evaluation, it is herewith noted that the wt.% of Cloister 20 nanoclay is having a major influence on the tensile modulus, subsequently followed by the wt.% of E-glass fiber and wt.% of Cloister 20 nanoclay.

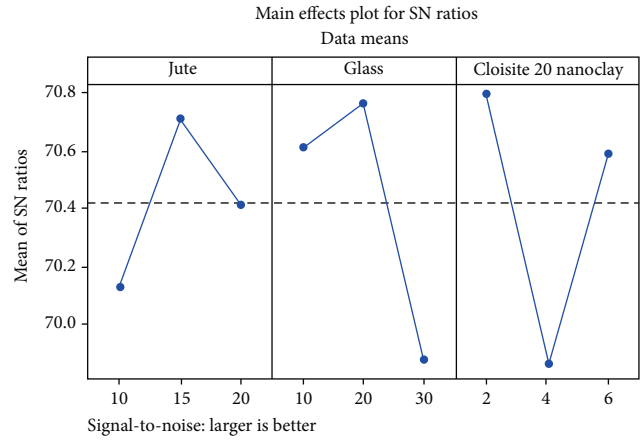

Figure 8: Main effects plot for SN ratios for tensile modulus.

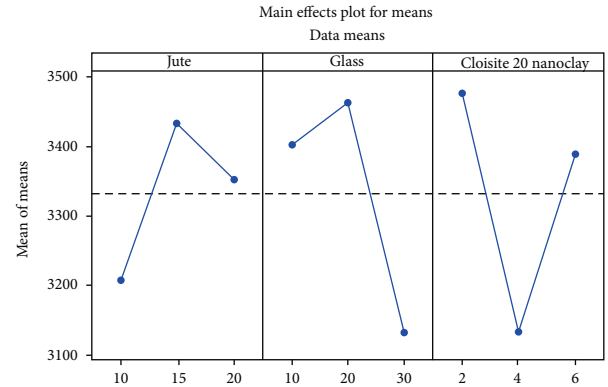

Figure 9: Main effects plot for means for tensile modulus.

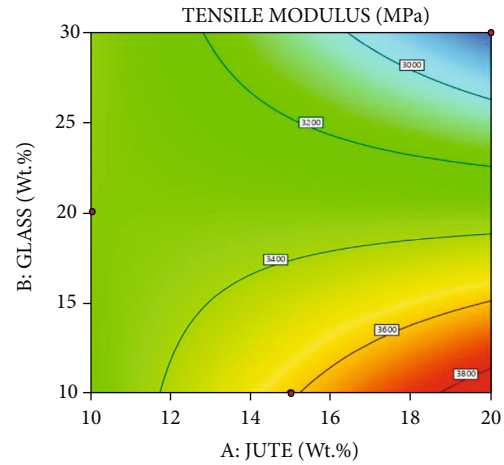

Figure 10: Surface plots for tensile modulus for varying wt.% of jute and E-glass fiber for 2 wt.% nanofiller (optimized wt.%).

Figure 8 gives the main effects plot for SN ratios, while Figure 9 gives the main effects plot for means. The main effects plot for SN ratios and the mean of means clearly indicate that the control factors can be optimally discerned with the level 2 of wt.% of jute (A2), level 2 of wt.% of E-glass

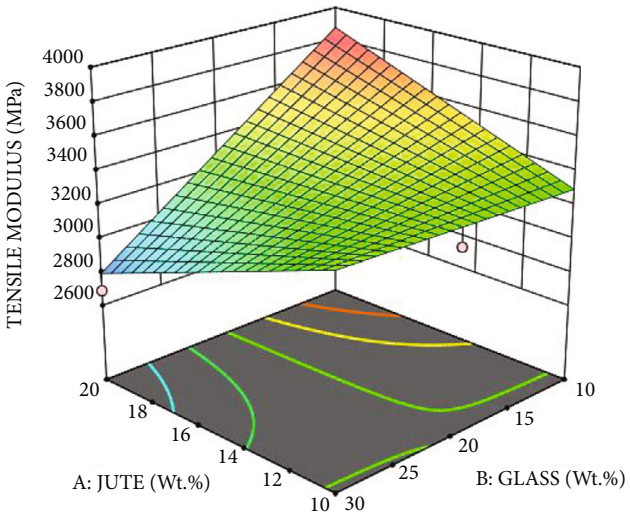

Figure 11: 3D contour plot for tensile modulus for varying wt.% of jute and E-glass fiber for 2 wt.% nanofiller (optimized wt.%).

Table 8: Results of the flexural test.

Specimen designation	Jute (wt.%)	E-glass (wt.%)	wt.% of Cloisite 20 nanoclay (wt. %)	Flexural strength (MPa)	Flexural modulus (MPa)
S1	10	10	2	74.89	117.56
S2	10	20	4	76.52	119.65
S3	10	30	6	79.56	121.89
S4	15	10	4	78.36	123.56
S5	15	20	6	80.56	124.89
S6	15	30	2	82.45	126.59
S7	20	10	6	83.21	127.31
S8	20	20	2	85.15	275.15
S9	20	30	4	90.22	261.33

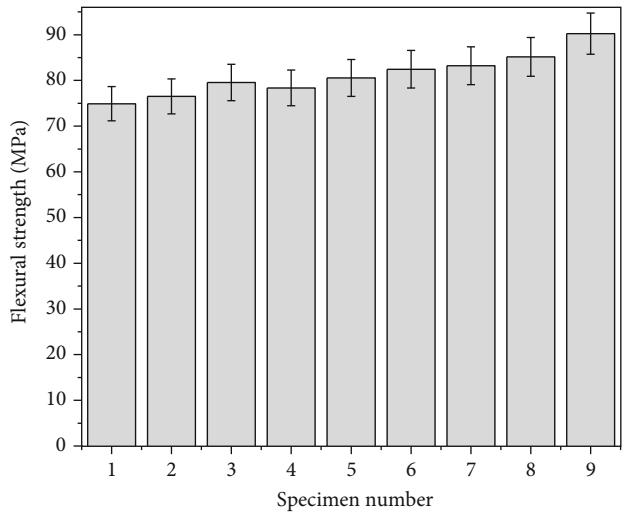

Figure 12: Flexural strength for prepared specimens.

Table 9: Response table for signal to noise (S/N) ratios for flexural strength.

Level	Jute (wt.%)	E-glass fiber (wt.%)	Cloisite 20 nanoclay (wt.%)
1	37.73	37.92	38.14
2	38.11	38.13	38.22
3	38.70	38.48	38.18
Delta	0.98	0.56	0.08
Rank	1	2	3
Larger is better			

Table 10: Response table for means for flexural strength.

Level	Jute (wt.%)	E-glass fiber (wt.%)	Cloisite 20 nanoclay (wt.%)
1	76.99	78.82	80.83
2	80.46	80.74	81.70
3	86.19	84.08	81.11
Delta	9.20	5.26	0.87
Rank	1	2	3

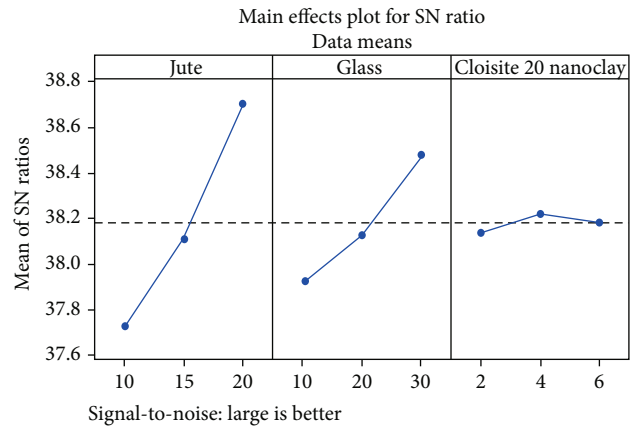

Figure 13: Main effects plot for SN ratios for flexural strength.

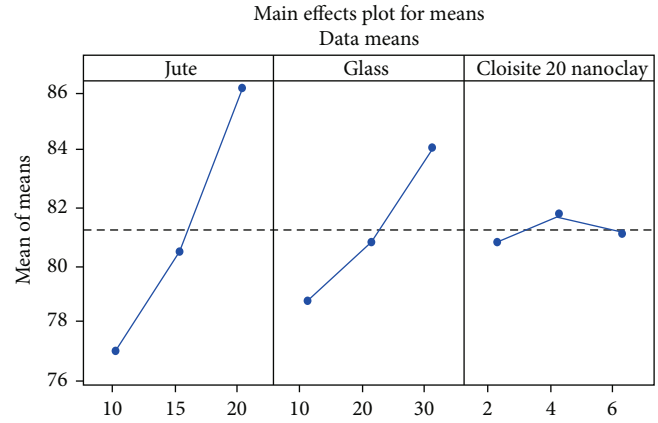

Figure 14: Main effects plot for means for flexural strength.

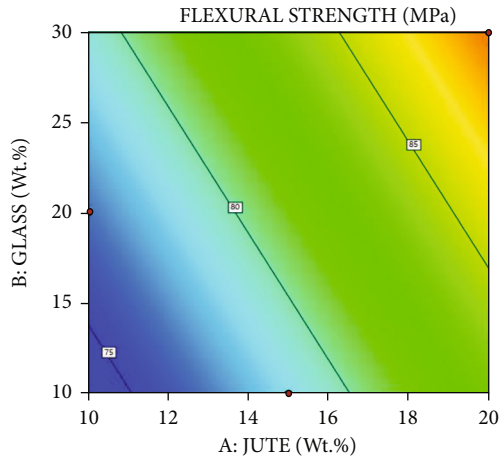

Figure 15: Surface plots for flexural strength for varying wt.% of jute and E-glass fiber for 4 wt.% nanofiller (optimized wt.%).

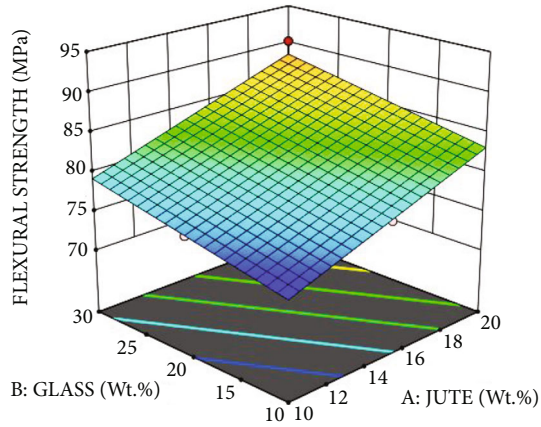

Figure 16: 3D contour plot for flexural strength for varying wt.% of jute and E-glass fiber for 4 wt.% nanofiller (optimized wt.%).

Table 11: Response table for signal to noise (S/N) ratios for flexural modulus.

Level	Jute (wt.%)	E-glass fiber (wt.%)	Cloisite 20 nanoclay (wt.%)
1	41.56	41.78	44.08
2	41.94	44.09	43.91
3	46.41	44.04	41.92
Delta	4.85	2.31	2.17
Rank	1	2	3
Larger is better			

fiber (B2), and level 1 of wt.% of Cloister 20 nanoclay (C1). Thus, the S/N ratio and mean of means analysis suggests that the A2, B2, and C1 are the optimum levels for maximizing the tensile modulus for the hybrid polymer composites.

Further, the main effects plot for means as shown in Figure 8 gives an overview of the means for the combination

Table 12: Response table for means for flexural modulus.

Level	Jute (wt.%)	E-glass fiber (wt.%)	Cloisite 20 nanoclay (wt.%)
1	119.7	122.8	173.1
2	125.0	173.2	168.2
3	221.3	169.9	124.7
Delta	101.6	50.4	48.4
Rank	1	2	3

of the control factors considered in the design of experiments for maximizing the tensile modulus of the composite specimens. The response (tensile modulus) and control factors are considered to model the influence of factors. From the statistical modeling of the responses and factors, equation (3) is obtained, which can be effectively used to predict the tensile modulus for different wt.% of reinforcements and the filler content.

$$\text{Tensile Modulus (MPa)} = \exp\left(Y'\right),$$

$$Y' = 8.1525 + 0.00436 * \text{Jute (wt.\%)} - 0.004000 * \text{E-Glass Fiber (wt.\%)} - 0.00682 * \text{Cloisite 20 Nanoclay (wt.\%)}. \quad (3)$$

Figures 10 and 11 give the surface and 3D contour plots for the varying wt.% of reinforcements for 2 wt.% of Cloister 20 nanoclay (optimized wt.%). It is evident from the graphs that the tensile modulus increase in the range of 3000 MPa to 3800 MPa up to 20 wt.% of jute fiber and 20 wt.% of E-glass fiber, beyond which there is a drastic decrease in the tensile modulus owing to microcoring and aggregation and also agglomeration of the nanofiller at some localized regions and uneven dispersion in the matrix, thus decreasing the load carrying capacity of the composites with the increase in the fiber reinforcements content beyond 20 wt.%.

3.4. Flexural Test. A three-point bending test was used in this research work to investigate the flexural properties of composite laminates on a universal testing machine in accordance with the ASTM D790 standards. The flexural strength and flexural modulus of the hybrid composites show a remarkable improvement owing to the improvement in the load carrying capacity along the transverse direction. It also shows that combining natural fibers with glass fibers expands the flexural capabilities. The hybridization of jute with glass fiber (S9) was discovered to have higher flexural strength with results of 90.22 MPa and higher flexural modulus with results of 275.15 MPa, for S8 specimen correspondingly. All of these findings show that the flexural characteristics of laminates are influenced not only by the hybrid ingredients but also by the laminate stacking sequence. Glass with high strength and stiffness are used as skin plies, which improves flexural and tensile qualities. Table 8 gives the experimental results of the flexural test. Figure 12 shows the flexural strength calculated for each specimen.

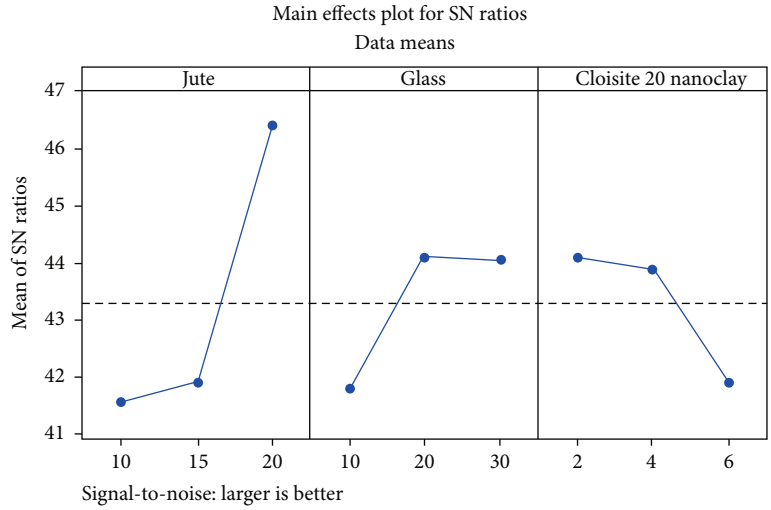

Figure 17: Main effects plot for SN ratios for flexural modulus.

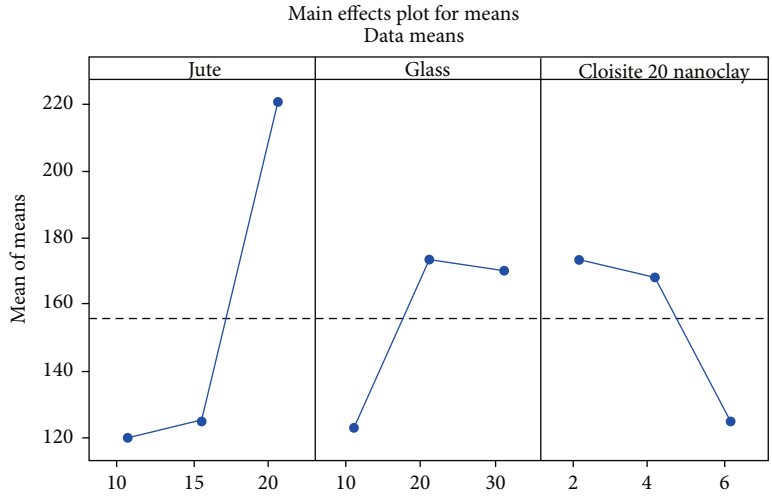

Figure 18: Main effects plot for means for flexural modulus.

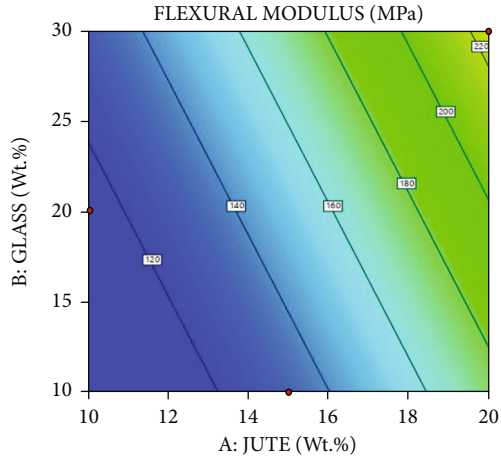

Figure 19: Surface plots for flexural modulus for varying wt.% of jute and E-glass fiber for 2 wt.% nanofiller (optimized wt.%).

3.5. Flexural Strength. The flexural strength is an important attribute of the polymer composite materials. The flexural strength gives the measure of the composite materials to withstand bending and is thus an important factor for the use of polymer composites in components subjected to bending stresses. In the present work, the flexural strength is found to be maximum (90.22 MPa) for S9 composite specimens (20 wt.% jute fiber and 30 wt.% E-glass fiber with 4 wt.% nanofiller). This is also ascertained from the statistical validations. The response table for SN ratios as shown in Table 9 and means as shown in Table 10 for flexural strength is critically evaluated, and from the evaluation, it is herewith noted that the wt.% of jute fiber is having a major influence on the flexural strength, subsequently followed by the wt.% of E-glass fiber and wt.% of Cloisite 20 nanoclay.

Figure 13 gives the main effects plot for SN ratios, while Figure 14 gives the main effects plot for means. The main effects plot for SN ratios and the mean of means clearly

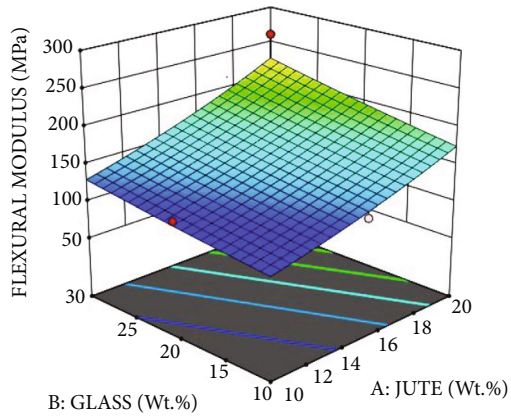

Figure 20: 3D contour plot for flexural modulus for varying wt.% of jute and E-glass fiber for 2 wt.% nanofiller (optimized wt.%).

Table 13: Results of the impact test.

Specimen designation	Jute (wt.%)	Glass (wt.%)	Cloisite 20 nanoclay (wt.%)	Impact strength (J/m^2)
S1	10	10	2	145.89
S2	10	20	4	146.59
S3	10	30	6	147.56
S4	15	10	4	149.65
S5	15	20	6	151.65
S6	15	30	2	152.45
S7	20	10	6	153.24
S8	20	20	2	178.26
S9	20	30	4	162.25

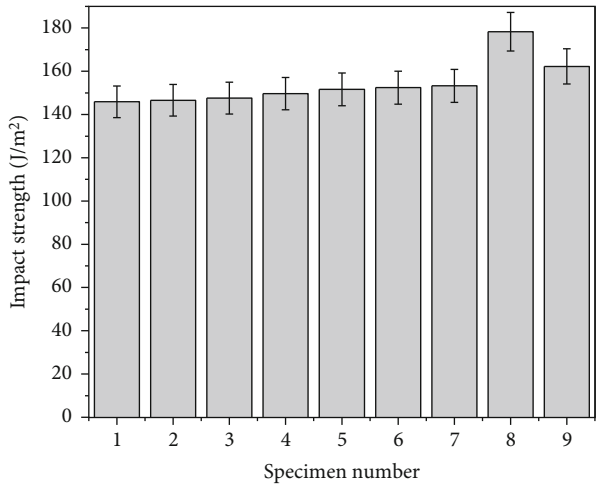

Figure 21: Impact strength for specimens.

indicate that the control factors can be optimally discerned with the level 3 of wt.% of jute (A3), level 3 of wt.% of E-glass fiber (B3), and level 2 of wt.% of Cloisite 20 nanoclay (C2). Thus, the *S*/*N* ratio and mean of means analysis suggests that the A3, B3, and C2 are the optimum levels for maximizing the flexural strength.

Table 14: Response table for signal to noise (*S*/*N*) ratios for impact strength.

Level	Jute	Glass fiber	wt.% of Cloisite 20 nanoclay
1	43.33	43.50	43.99
2	43.59	43.99	43.68
3	44.31	43.75	43.57
Delta	0.98	0.49	0.42
Rank	1	2	3
Larger is better			

Table 15: Response table for means for impact strength.

Level	Jute (wt.%)	Glass fiber (wt.%)	Cloisite 20 nanoclay (wt.%)
1	146.7	149.6	158.9
2	151.3	158.8	152.8
3	164.6	154.1	150.8
Delta	17.9	9.2	8.0
Rank	1	2	3

Further, the response (flexural strength) and control factors are considered to model the influence of factors. From the statistical modeling of the responses and factors, equation (4) is obtained, which can be effectively used to predict the tensile modulus for different wt.% of reinforcements and the filler content.

$$\text{Flexural Strength (MPa)} = \exp\left(Y'\right)$$

$$Y' = 4.155 + 0.01135 * \text{Jute (wt.\%)} + 0.00324 * \text{E-Glass Fiber (wt.\%)} + 0.0013 * \text{Cloisite 20 Nanoclay (wt.\%)}. \quad (4)$$

Figures 15 and 16 give the surface and 3D contour plots for the varying wt.% of reinforcements for 4 wt.% of Cloister 20 nanoclay (optimized wt.%). It is evident from the graphs that the flexural strength increases in the range of 75 MPa to 90 MPa with the increase in the wt.% of jute (20 wt.%) and E-glass fiber (30 wt.%). This is attributed to the strengthened network of the reinforcements in the matrix resisting the fracture of the surfaces due to the bending. The nanofiller further adds to the strengthening of the composites.

3.6. Flexural Modulus. The flexural modulus is an important parameter for evaluating the flexural stiffness of the composite. In the present work, the flexural modulus is found to be maximum at 275.15 MPa for the S8 specimen (20 wt.% jute fiber, 30 wt.% of E-glass fiber with 2 wt.% Cloisite 20 nanoclay). This is also ascertained from the response tables and plots for SN ratios and means. The response table for SN ratios as shown in Table 11 and means as shown in Table 12 for flexural modulus is critically evaluated, and

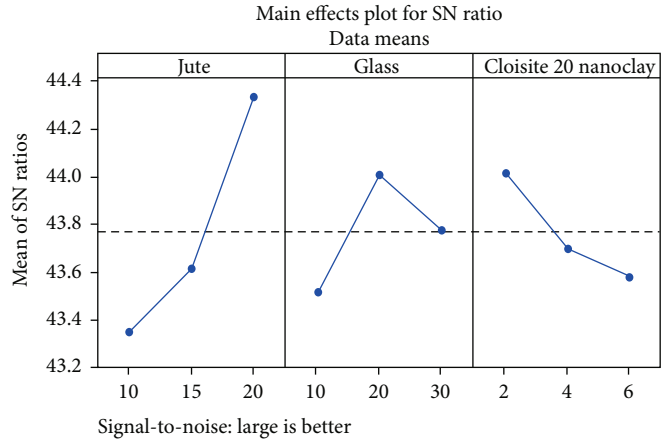

Figure 22: Main effects plot for SN ratios for impact strength.

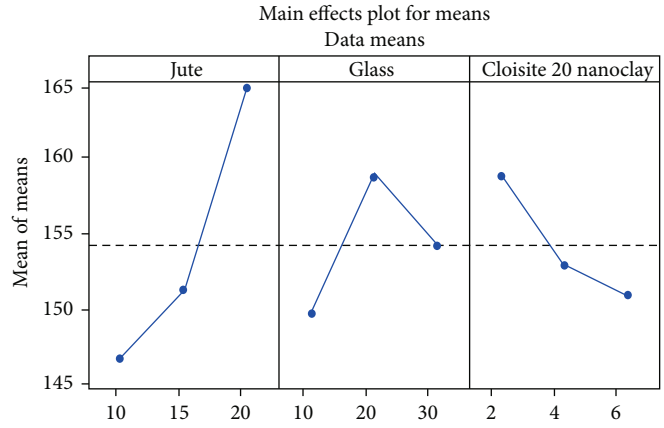

Figure 23: Main effects plot for means for impact strength.

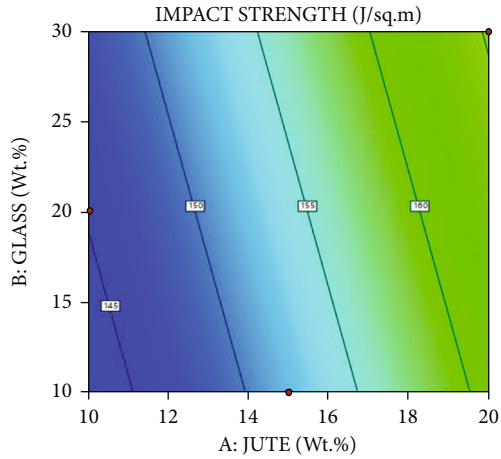

Figure 24: Surface plots for varying wt.% of jute and E-glass fiber for 2 wt.% nanofiller (optimized wt.%).

from the evaluation, it is herewith noted that the wt.% of jute fiber is having a major influence on the flexural modulus, subsequently followed by the wt.% of E-glass fiber and wt.% of Cloisite 20 nanoclay.

The findings of Ravichandran et al. [33] have also revealed that the inclusion of the nanofiller will enhance the flexural strength and flexural modulus of the composite specimens, since the nanofiller will act as inoculants and improve the bonding strength of the composite specimens, and thereby, the flexural characteristics of the composites are found to improve. That is, the flexural strength has increased from 379 MPa to 534.9 MPa for the HNT filler-based glass fiber-reinforced polymer composite with an improvement of 41.13%, subsequently followed by an improvement in the flexural modulus by 39%.

Figure 17 gives the main effects plot for SN ratios, while Figure 18 gives the main effects plot for means. The main effects plot for SN ratios and the mean of means clearly indicate that the control factors can be optimally discerned with the level 3 of wt.% of jute (A3), level 2 of wt.% of E-glass fiber (B2), and level 1 of wt.% of Cloisite 20 nanoclay (C1). Thus, The *S*/*N* ratio and mean of means analysis suggests that the A3, B2, and C1 are the optimum levels for maximizing the flexural modulus for the hybrid polymer composites.

Further, the response (flexural modulus) and control factors are considered to model the influence of factors. From the statistical modeling of the responses and factors, equation (5) is obtained, which can be effectively used to predict

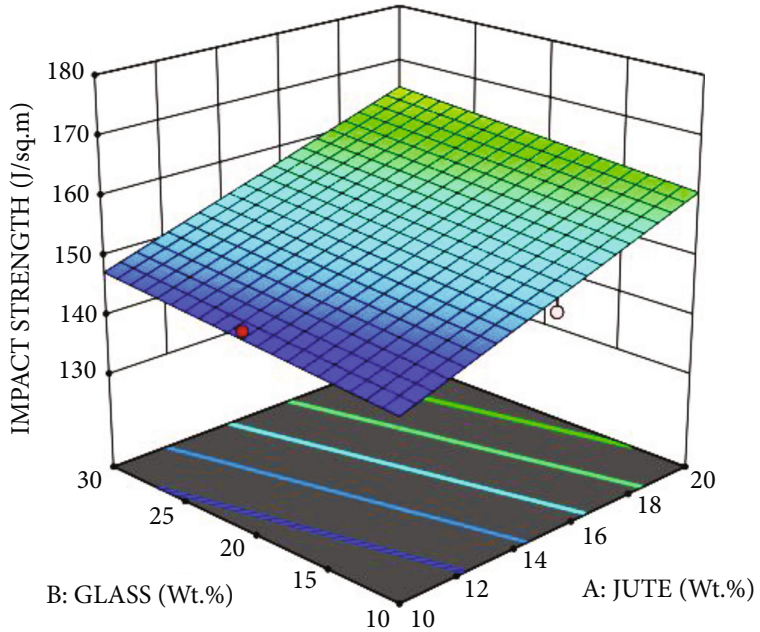

Figure 25: 3D contour plot for varying wt.% of jute and E-glass fiber for 2 wt.% nanofiller (optimized wt.%).

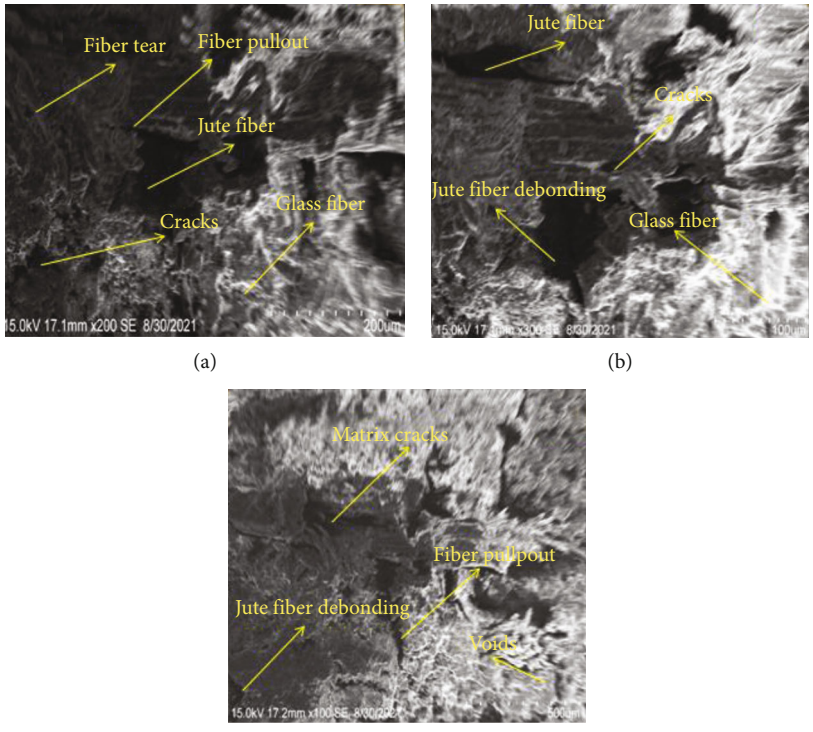

(a) (b)

(c)

Figure 26: The fractured surfaces of the hybrid composite for the tensile test under different fiber loading of specimens: (a) S1, (b) S4, and (c) S7.

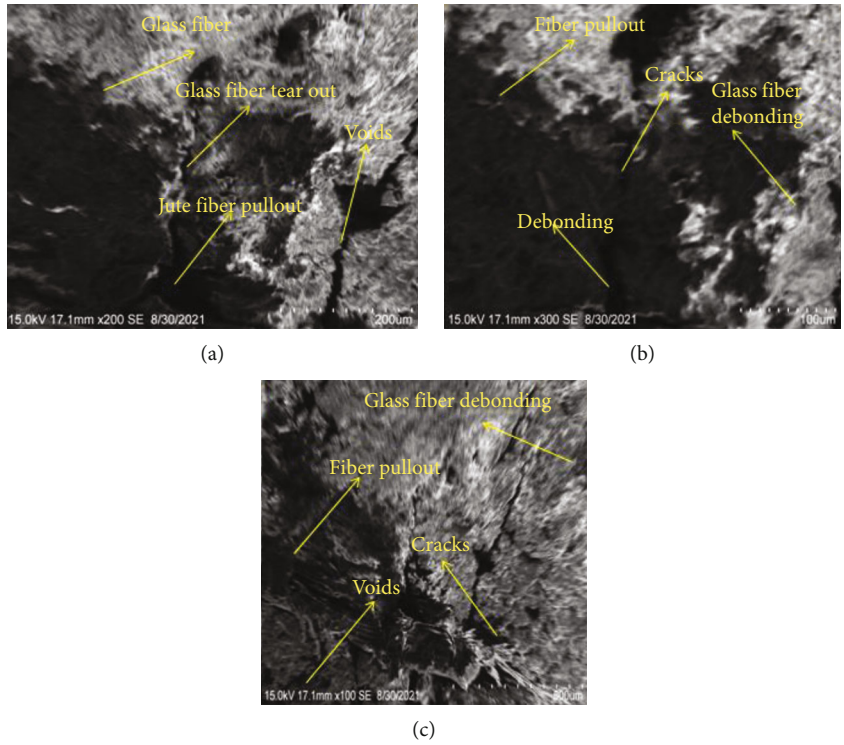

Figure 27: Fractured surfaces of the hybrid composite for the flexural test under different fiber loading of specimens: (a) S4, (b) S7, and (c) S9.

the tensile modulus for different wt.% of reinforcements and the filler content.

$$\text{Flexural Modulus (MPa)} = \exp\left(Y'\right),$$

$$Y' = 4.030 + 0.06507 * \text{Jute (wt.\%)} + 0.01333 * \text{E-Glass Fiber (wt.\%)} - 0.0690 * \text{Cloisite 20 Nanoclay (wt.\%)}. \quad (5)$$

Figures 19 and 20 give the surface and 3D contour plots for the varying wt.% of reinforcements for 2 wt.% of Cloister 20 nanoclay (optimized wt.%). It is evident from the graphs that the flexural modulus increases in the range of 120 MPa to 220 MPa with the increase in the wt.% of jute (20 wt.%) and E-glass fiber (30 wt.%). However, with the increase in the wt.% of filler content beyond 2 wt.%, the flexural modulus decreases due to the microcoring and segregation of the filler along the transverse direction, thereby leading to the reduction in the flexural modulus of the composite specimens.

3.7. Impact Test. The Charpy impact test is utilized to study the influence of reinforcements on the impact characteristics of various specimens. The impact strength is determined utilizing the Charpy impact machine's reading. The hardness of a material is determined via impact tests. Normally, man-made fibers form boundary having minor force with resin due to which force preoccupation rises at these boundaries. A usual fiber displays stronger fiber/matrix force which does not permit force to be fascinated at interface. The investigations on the Charpy impact test have demonstrated that minor addition of jute fiber has enhanced the connection competence and expands the area under the stress-strain curve and creates stronger impact strength. Taken together, the quantity of jute, which is further fragile than glass fiber, drastically affects the impact strength of the composites. The investigation findings of impact testing of composites with varied weight percentage of reinforcement are provided in Table 13. The testing revealed that composites manufactured with 20 wt.% of jute and 20 wt.% of E-glass fiber exhibited greater strength with 2 wt.% of Cloisite 20 nanoclay. The reason for this is that natural fiber has larger cellulose content and a smaller microfibril angle, which results in a superior fracture resistance for impact loading. Figure 21 represents the impact strength of the specimens.

The response table for SN ratios as shown in Table 14 and means as shown in Table 15 for impact strength is critically evaluated, and from the evaluation, it is herewith noted that the wt.% of jute fiber is having a major influence on the impact strength, subsequently followed by the wt.% of E-glass fiber and wt.% of Cloisite 20 nanoclay.

Figure 22 gives the main effects plot for SN ratios, while Figure 23 gives the main effects plot for means. The main effects plot for SN ratios and the mean of means clearly indicate that the control factors can be optimally discerned with the level 3 of wt.% of jute (A3), level 2 of wt.% of E-glass fiber (B2), and level 1 of wt.% of Cloister 20 nanoclay (C1). Thus, the *S*/*N* ratio and mean of means analysis suggests that the A3, B2, and C1 are the optimum levels for maximizing the impact strength for the hybrid polymer composites.

Further, the response (flexural modulus) and control factors are considered to model the influence of factors. From the statistical modeling of the responses and factors, equation (6) is obtained, which can be effectively used to predict the tensile modulus for different wt.% of reinforcements and the filler content.

$$\text{Impact Strength}\left(\text{J/m}^2\right) = \exp\left(Y'\right),$$

$$Y' = 4.887 + 0.01158 * \text{Jute (wt, \%)} + 0.00138 * \text{E-Glass Fiber (wt.\%)} - 0.0129 * \text{Cloisite 20 Nanoclay (wt.\%)}. \quad (6)$$

Figures 24 and 25 give the surface and 3D contour plots for the varying wt.% of reinforcements for 2 wt.% of Cloisite 20 nanoclay (optimized wt.%). It is evident from the graphs that the impact strength increases in the range of 145 MPa to 160 MPa with the increase in the wt.% of jute (20 wt.%) and E-glass fiber (30 wt.%). However, with the increase in the wt.% of filler content beyond 2 wt.%, the impact strength decreases owing to the decrease in the area under the stress-strain curve due to homogenized distribution of the reinforcements and filler material, thereby reducing the ability of the composites to store the energy before the failure under impact load.

3.8. Microscopy. The SEM setup was utilized to look at the interfacial properties of UV-treated and untreated fiber composites. Figure 26 shows the tensile fractured surface of uncovered jute/glass hybrid composites for S1, S4, and S7 specimens. In light of the significant variety in compound and actual properties, just as the production of hydrogen connections between untreated glass and jute fiber, the fiber agglomerates into groups and turns out to be unevenly scattered in the matrix. Thus, the untreated composite has more noteworthy pullout. Figure 27 shows the ductile breaking surfaces of ideal UV-treated base hybrid composites for S3, S6, and S9 specimens. At the point when glass and jute are all UV-treated, better dispersion and modulus of rupture of the filaments from the framework are seen at ideal powers and hybridized at ideal proportions (1 : 3). As demonstrated in Figure 26, actual change of the strands, for example, no ionizing UV radiation, hinders hydrogen security development and builds the quantity of free extreme dynamic locales, bringing about expanded scattering and interfacial holding. The composites treated during tensile and impact tests were observed under a SEM in the postcrack condition. In the SEM pictures shown, the fiber dispersion is easily visible. At a magnification of 500 times, the fibers, as well as the fiber agglomeration and matrix without fiber, are clearly evident in Figure 26(a)). The atmosphere holes are detectable in Figure 26(c), as seen in the illustration. Figures 26(a), 26(b), 27(a) and 27(b), show how these air gaps affect the composite's strength. Figure 27(b) shows severe fiber pullout on the tension side of the fracture, indicating that no outline of matrix resin is stuck to the fiber, indicating poor fiber matrix adhesion and a significant reduction in composite strength. Fiber agglomerations and fiber pullout are depicted in Figure 27(a). Figure 27(b) also demonstrates the debonding of the fibers from the matrix. Further, Figure 27(c) depicts the agglomeration owing to the stacking or gathering of fibers in a matrix, which decreases strength due to nonstandardized stress transmit. Fiber matrix bond, fiber dispersal and direction, fiber aggregation, and the existence of air voids are all factors that might cause a fiber-reinforced composite's strength to be reduced.

4. Conclusion

The experimental and mechanical performance of reinforced glass and glass/jute fiber polyester-based hybrid composites was experimentally investigated. The following results can be taken from the preceding study:

(i) A hybrid composite was successfully made, which was fortified with both glass and jute fibers

(ii) The current research indicates that integrating various fiber loads into the polyester matrix with varying weight percentages increases various composite properties

(iii) The maximum tensile, flexural, and impact resistance is exhibited by a composite reinforced with 30% of fiber. The mechanical performance is improved for all other composites of varying weight ratios of fiber loads. Both synthetic (GF) and natural (JF) fibers can be integrated into the polyester matrix to improve some properties

(iv) In the future, investigators would have greater benefit and scope to study the current area of science. Other dimensions of these composites including thermal, morphological, and mechanical dynamic characteristics can be investigated using the findings of this analysis. Different natural fibers with different fiber loads and injection moldings will further alter this function

(v) The hybrid composites with 20 wt.% of jute and 20 wt.% of E-glass fiber and 2 wt.% of Cloisite 20 nanoclay (S8) have optimum tensile strength of 69.7 MPa, tensile modulus of 3816.43 MPa, and flexural modulus of 275.15 MPa. The flexural strength of the composite is maximum for the S9 specimen (20 wt.% of jute, 30 wt.% of E-glass fiber, and 4 wt.% of Cloisite nanoclay) with a value of 90.22 MPa. The maximum value of impact strength of the hybrid composite specimen is 178.62 J/m^2 for the S8 specimen. This improvement in the properties is due to the strong bonding between the jute fiber, the glass fiber, and the polyester matrix material, brought about by the Cloisite 20 nanoclay filler material

(vi) The jute/glass fiber-reinforced composites appeared to perform substantially better. According to the findings, hybrid composites displayed superior tensile and flexural characteristics. The findings of this study show that jute/glass hybrid composites have greater mechanical qualities, making them more

suitable for automotive applications. These findings are also ascertained from Taguchi's optimization and predictions. Statistical models are developed to predict the variation of the mechanical properties of these hybrid composites and are validated. As a result of this conclusion, it is certain that the hybrid composites with jute and E-glass fiber can be used for better strength-bearing capabilities

Data Availability

The data used to support the findings of this study are included within the article. Further data or information is available from the corresponding author upon request.

Conflicts of Interest

The authors declare that there is no conflict of interest regarding the publication of this article.

Acknowledgments

The authors appreciate the supports from Haramaya University, Dire Dawa, Ethiopia, for providing help during the research and preparation of the manuscript. The authors thank Nitte Meenakshi Institute of Technology, MVJ College of Engineering, Bangalore Institute of Technology, and Dr. Sivanthi Aditanar College of Engineering for providing assistance to complete this work.

References

[1] A. K. Kaw, *Mechanics of Composite Materials*, CRC PRESS Taylor & Francis Group, 2nd edition, 2006.

[2] A. G. Facca, M. T. Kortschot, and N. Yan, "Predicting the elastic modulus of natural fiber reinforced thermoplastics," *Composites: Part A: Applied Science and Manufacturing*, vol. 37, pp. 1660–1671, 2006.

[3] D. N. Saheb and J. P. Jog, "Natural fiber polymer composites: a review," *International catalogue of scientific literature [Schedule of classification]*, vol. 18, no. 4, pp. 351–363, 1999.

[4] D. P. Archana, H. N. Jagannatha Reddy, N. Jeevan, R. Prabhakara, M. U. Aswath, and B. Paruti, "Natural jute fibre-reinforced polymer composite system for posttensioned beam strengthening in flexure," *Advances in Materials Science and Engineering*, vol. 2021, Article ID 2905150, 14 pages, 2021.

[5] J. Kasama and S. Nitinat, "Effect of glass fiber hybridization on properties of sisal fiber polypropylene composites," *Composites Part B: Engineering*, vol. 40, no. 7, pp. 623–627, 2009.

[6] R. Malkapuram, V. Kumar, and Y. S. Negi, "Recent development in natural fiber reinforced polypropylene composites," *Journal of Reinforced Plastics and Composites*, vol. 28, pp. 1169–1189, 2009.

[7] S. Harish, D. Peter Michael, A. Bensely, D. Mohan Lalb, and A. Rajadurai, "Mechanical property evaluation of natural fiber coir composite," *Materials Characterization*, vol. 60, no. 1, pp. 44–49, 2009.

[8] G. Raghavendra, S. Ojha, S. K. Acharya, and S. K. Pal, "A comparative analysis of woven jute/glass hybrid polymer composite with and without reinforcing of fly ash particles," *Polymer Composites*, vol. 37, no. 3, 2016.

[9] S. Raghavendra, K. N. Manjunatha, and C. S. Anjinappa, "Thermo mechanical characteristics of sisal fibre reinforced composites after treatment with potassium permanganate and stearic acid," *Journal of materials and Engineering Structures*, vol. 9, pp. 99–105, 2022.

[10] M. A. Rahuman, S. S. Kumar, R. Prithivirajan, and S. Gowri Shankar, "Dry sliding wear behavior of glass and jute fiber hybrid reinforced epoxy composites," *International Journal of Engineering Research and Development*, vol. 10, no. 11, pp. 46–50, 2014.

[11] D. P. Archana, H. N. Jagannatha Reddy, R. Prabhakara, M. U. Aswath, and A. Chandrashekar, "Processing and properties of biodegradable composites to strengthen structures," *Journal of The Institution of Engineers (India): Series C*, vol. 103, no. 1, pp. 39–52, 2022.

[12] M. Rokbi, H. Osmania, A. Imad, and N. Benseddiq, "Effect of chemical treatment on flexure properties of natural fiber-reinforced polyester composite," *Procedia Engineering*, vol. 10, pp. 2092–2097, 2011.

[13] M. Ramesh, K. Palanikumar, and K. Hemachandra Reddy, "Mechanical property evaluation of sisal–jute– glass fiber reinforced polyester composites," *Composites Part B: Engineering*, vol. 48, pp. 1–9, 2013.

[14] M. Pinto, V. B. Chalivendra, Y. K. Kim, and A. F. Lewis, "Improving the strength and service life of jute/epoxy laminar composites for structural applications," *Composite Structures*, vol. 156, pp. 333–337, 2016.

[15] D. P. Archana and H. N. J. Reddy, "Potential of natural fibres for strengthening existing structures – a review," *International Journal of Structural Engineering and Analysis*, vol. 4, no. 2, 2018.

[16] M. Y. Khalid, Z. U. Arif, M. F. Sheikh, and M. A. Nasir, "Mechanical characterization of glass and jute fiber-based hybrid composites fabricated through compression molding technique," vol. 14, Tech. Rep. 5, , Int. J, Material Form, 2021.

[17] Z. M. Salisu, S. U. Ishiaku, D. Abdullahi, M. K. Yakubu, and B. H. Diyauddeen, "Development of kenaf shive bio–mop via surface deposit technique for water remediation from crude oil spill contamination," *Results in Engineering*, vol. 3, article 100020, 2019.

[18] P. A. Bonnet-Masimbert, F. Gauvin, H. J. H. Brouwers, and S. Amziane, "Study of modifications on the chemical and mechanical compatibility between cement matrix and oil palm fibres," *Results in Engineering*, vol. 7, article 100150, 2020.

[19] K. Aworinde, S. O. Adeosun, F. A. Oyawale, E. T. Akinlabi, and S. A. Akinlabi, "Comparative effects of organic and inorganic bio-fillers on the hydrophobicity of polylactic acid," *Results in Engineering*, vol. 5, article 100098, 2020.

[20] S. O. Odeyemi, R. Abdulwahab, A. G. Adeniyi, and O. D. Atoyebi, "Physical and mechanical properties of cement-bonded particle board produced from African balsam tree (Populous balsamifera) and periwinkle shell residues," *Results in Engineering*, vol. 6, article 100126, 2020.

[21] M. Y. Khalid, A. Al Rashid, Z. U. Arif, N. Akram, H. Arshad, and F. P. Garcia Marquez, "Characterization of failure strain in fiber reinforced composites: under on-axis and off-axis loading," *Crystals*, vol. 11, no. 2, p. 216, 2021.

[22] A. C. Pereira, S. N. Monteiro, F. S. de Assis, F. M. Margem, F. S. da Luz, and F. de Oliveira Braga, "Charpy impact tenacity of epoxy matrix composites reinforced with aligned jute fibers," *Journal of Materials Research and Technology*, vol. 6, no. 4, pp. 312–316, 2017.

[23] A. Ali, M. A. Nasir, M. Y. Khalid et al., "Experimental and numerical characterization of mechanical properties of carbon/jute fabric reinforced epoxy hybrid composites," *Journal of Mechanical Science and Technology*, vol. 33, no. 9, pp. 4217–4226, 2019.

[24] S. N. Monteiro, A. C. Pereira, C. L. Ferreira, E. Pereira Júnior, R. P. Weber, and F. S. de Assis, "Performance of plain woven jute fabric-reinforced polyester matrix composite in multilayered ballistic system," *Polymers*, vol. 10, no. 3, p. 230, 2018.

[25] A. V. Seetha Girish, B. Vijaya, S. Arjun, and S. Raghavendra, "Manufacturing and mechanical characterization of coir fibre composites based vinyl ester," *Advances in Materials and Processing Technologies*, pp. 1–10, 2021.

[26] R. Gujjala, S. Ojha, S. K. Acharya, and S. K. Pal, "Mechanical properties of woven jute– glass hybrid-reinforced epoxy composite," *Journal of Composite Materials*, vol. 48, no. 28, pp. 3445–3455, 2014.

[27] K. Palani Kumar, D. Keshavan, E. Natarajan et al., "Evaluation of mechanical properties of coconut flower cover fibre-reinforced polymer composites for industrial applications," *Progress in Rubber, Plastics and Recycling Technology*, vol. 37, no. 1, pp. 3–18, 2021.

[28] S. S. Patil, B. A. Praveen, U. N. Kempaiah, and H. Adarsha, "Fabrication and characterization of Kevlar/jute reinforced epoxy," *International Research Journal of Engineering and Technology*, vol. 4, no. 9, 2017.

[29] H. G. Anilthota and B. A. Praveena, "Processing and characterization of green composites using sisal and palm fibers," *International Journal of Engineering Science and Computing*, vol. 7, pp. 4262–4265, 2017.

[30] M. Korisidda, C. Prasad, and B. C. Mahantesh, "Study on mechanical properties of bio-composites," *International Journal for Scientific Research & Development*, vol. 6, no. 2, pp. 1–5, 2018.

[31] S. P. Yadav, V. K. Shankar, L. Avinash et al., "Development of 3D printed electromyography controlled bionic arm, sustainable machining strategies for better performance," in *Sustainable Machining Strategies for Better Performance*, pp. 11–21, Springer, Singapore, 2021.

[32] G. Ravichandran, G. Rathnakar, and N. Santhosh, "Effect of heat treated HNT on physico-mechanical properties of epoxy nanocomposites," *Composites Communications*, vol. 13, no. 2, pp. 42–46, 2019.

[33] G. Ravichandran, G. Rathnakar, N. Santhosh, and R. Suresh, "A Comparative study on the effect of HNT and nano-alumina particles on the mechanical properties of vacuum bag moulded glass-epoxy nano composites," *Mechanics of Advanced Composite Structures*, vol. 8, pp. 119–131, 2021.